Journal of Sound and Vibration (1999) **228**(2), 305–332
Article No. jsvi.1999.2413, available online at http://www.idealibrary.com on IDEAL®

VIBRATIONS OF BEAMS AND HELICES WITH ARBITRARILY LARGE UNIFORM CURVATURE

T. TARNOPOLSKAYA AND F. R. DE HOOG

CSIRO Mathematical and Information Sciences, Canberra, Australia

A. TARNOPOLSKY

Aerospace and Mechanical Engineering, ADFA, Canberra, Australia

AND

N. H. FLETCHER

Research School of Physical Sciences and Engineering, Australian National University, Canberra, Australia

(*Received* 11 *January* 1999, *and in final form* 19 *May* 1999)

An analytical, numerical, and experimental study of the vibrational modes of beams with constant curvature, ranging from small values up to helices with large numbers of turns, is presented. It is shown that, after an initial stage at low curvature in which extensional symmetrical modes hybridize so as to become inextensional, all modes show a decrease in frequency with increasing beam curvature. The frequency reaches a minimum at a value of the curvature which is a function of mode number and successive minima are separated by steps of π in the opening angle of the beam. For large values of curvature it is shown that, for both symmetric and antisymmetric modes, there are two types of vibrational modes with comparable frequencies. Modes develop into one or the other of these types in a way that is precisely defined but that has the appearance of being random. Physical descriptions of the processes involved are given, and the modes of the two types are described.

1. INTRODUCTION

The free in-plane vibration of beams with constant curvature has attracted the attention of researches since the last century [1–15] (for a detailed overview of the literature on the topic the reader is referred to review articles [10, 11]). The majority of the research has been devoted to the vibration of circular arches with opening angle up to π, and a more limited number to the vibration of incomplete rings with opening angle less than 2π. In the authors' previous papers [12, 14], a phenomenon of mode transition from extensional to inextensional that accompanies an increase in beam curvature and occurs at relatively small values of the beam opening angle has been examined. It has been observed that upon

0022-460X/99/470305 + 28 $30.00/0

completion of the mode transition, the frequencies of all modes decrease with increase in beam curvature. It was the purpose of the present paper to examine the changes in vibrational behaviour that take place with further increase in beam curvature. While the initial motivation of the study was to examine the behaviour of moderately curved vibrating foils in ultrasonic transducers, it has proved possible to apply the formalism developed to arbitrarily large curvature. Once the curvature has increased to an extent that the opening angle becomes greater than 2π, it is, of course, impossible to realize a strictly planar uniformly curved beam of this type. To an adequate approximation, however, a beam with large constant curvature can be treated as a helix, provided that the helical pitch is small compared with its diameter and that motion parallel to the helical axis is ruled out. Under these assumptions, the width of the beam is of no consequence, provided it is constant, but we assume the width to be very small compared with the radius of curvature so that the helix to which the beam is curved when the opening angle exceeds 2π has a very small pitch. In practical terms, the ratio of helical pitch to its diameter of about 1 : 10 and beams with width at least as large as 10 times their thickness are found to conform to the theory.

For long beams with very large constant curvature, our analysis converges towards some aspects of published work on helical springs [16–22]. The approach in such work is however generally very different from that employed here. Three-dimensional equations for vibration of helices are generally too difficult to solve analytically and most work reduces to the calculation of natural frequencies by various numerical techniques. The importance of simplified models that provide a deep insight into different effects inherent in helices vibration has long been recognized [19]. A simplified model presented in this paper considers a helix as a planar uniformly curved beam vibrating in the plane of the beam curvature and is essentially different from the published simplified models [16–19]. Although our model does not take into account the longitudinal vibration and is limited to a small helical pitch, it provides an insight into the association of the modes of a helix with the modes of a curved beam and it reveals that different types of helix modes in fact originate from the same type of the curved beam modes.

The analysis of this paper reveals that the non-dimensional eigenvalue and displacements are functions of beam opening angle only (which is a product of beam curvature and length), and therefore the changes in vibrational behaviour observed when the beam curvature is increased pertain equally to the case when the curvature is held constant while the length of the beam is increased. The transition from non-dimensional eigenvalue to natural frequency is straightforward, but it should be borne in mind that the frequency versus opening angle curves will be different for the case when the length of the beam is held constant while the curvature is increased and for the opposite case.

The analysis consists of two parts: (1) analysis of vibrational behaviour at relatively small opening angle (but larger than that encompassing the initial mode transition); and (2) analysis of vibrational behaviour at arbitrarily large opening angle. For both cases, simple analytic approximations for non-dimensional eigenvalue and mode shape are obtained. An interesting feature of the vibrational behaviour at smaller opening angle, revealed by the analysis, is the occurrence of

a minimum of the non-dimensional eigenvalue at a value of the opening angle that is a function of the mode number. This minimum relates to the minimum of strain energy. The analysis also reveals that there are two different types of vibrational behaviour at large opening angle, characterized by quite different mode shapes. These modes, and their succession in the frequency spectrum, are examined in detail and found to conform to simple rules.

Numerical calculations illustrating the vibrational behaviour at different ranges of opening angle and confirming the validity of the analytical approximations are presented and a physical interpretation of the forms of the various modes and their transitions is given.

Finally, the results of the analysis have been confirmed by the experiments with both moderately curved beams and helices with increasing numbers of turns.

2. GOVERNING EQUATIONS

As mentioned in the introduction, the equations of in-plane vibration of a uniformly curved beam with large opening angle give an appropriate approximation for the vibration of a helix, provided that the helical pitch is small compared with its diameter and that the motion in the direction of the helical axis is neglected. The equations of free in-plane vibration of a uniformly curved beam can be found in many sources [1–14]. We have used the non-dimensional form of the equations given in [12]:

$$(u' - \alpha v)' + \varepsilon \Lambda u = 0, \tag{1}$$

$$-\varepsilon(\alpha^4 v + 2\alpha^2 v'' + v'''') + (u' - \alpha v)\alpha + \varepsilon \Lambda v = 0, \tag{2}$$

where u and v are the non-dimensional tangential and normal displacements, α is the opening angle, which is the ratio of beam length l to its radius of curvature R, Λ is a non-dimensional eigenvalue and ε is a slenderness parameter of the beam, defined by

$$\Lambda = \frac{\rho l^2 \omega^2}{\varepsilon E}, \tag{3}$$

$$\varepsilon = \frac{h^2}{12 l^2}, \tag{4}$$

where h is the beam thickness, ρ is the density, E is Young's modulus and ω is the frequency. Primes denote differentiation with respect to the non-dimensional coordinate $\bar{s} = s/l$ measured along the beam centreline. In these equations, rotational inertia effects have been neglected. It is also assumed that the beam has rectangular cross-section, but it is straightforward to generalize the results of this paper for other forms of cross-section. We also assume that the ends of the beam are

clamped, so that

$$u = 0 \quad \text{at } \bar{s} = 0, 1, \tag{5}$$

$$v = v' = 0 \quad \text{at } \bar{s} = 0, 1. \tag{6}$$

3. ANALYSIS OF THE EQUATIONS

In this section, we present an analysis of the equations of free vibration of beams with constant curvature. Firstly, we show that at large opening angle these equations can be approximated with sufficient accuracy by the equations of inextensional vibrations. We then derive analytical approximations for two cases: for relatively small opening angle and for large opening angle. Finally, we compare the analytical approximations with numerical solutions.

3.1. APPROXIMATION FOR EQUATIONS

In order to show that equations (1, 2) can be approximated by the equations of inextensional vibration, it is convenient to reduce equations (1, 2) to a single equation in terms of the transverse displacement v only. Differentiating equation (1), multiplying equation (2) by α and subtracting them yields

$$(u' - \alpha v)'' + (u' - \alpha v)(\Lambda\varepsilon - \alpha^2) + \varepsilon\alpha(\alpha^4 v + 2\alpha^2 v'' + v'''') = 0. \tag{7}$$

Substituting for $u' - \alpha v$ from equation (2) gives

$$v'''''' + 2\alpha^2 v'''' + (\alpha^4 - \Lambda)v'' + \Lambda v\alpha^2 + \varepsilon[\Lambda(\alpha^4 v + 2\alpha^2 v'' + v'''' - \Lambda v)] = 0. \tag{8}$$

The boundary conditions (5, 6) can also be rewritten in terms of the transverse displacement v. Expressing u from equation (1) and substituting for $u' - \alpha v$ from equation (2) gives

$$u = \frac{\varepsilon(\alpha^4 v' + 2\alpha^2 v''' + v'''''') - \Lambda\varepsilon v'}{\alpha\varepsilon\Lambda}. \tag{9}$$

The boundary condition (5) can be expressed in terms of the transverse displacement v by substituting the boundary conditions (5) and (6) into equation (9):

$$v'''''' + 2\alpha^2 v''' = 0 \quad \text{at } \bar{s} = 0, 1. \tag{10}$$

When the opening angle α is sufficiently large, the non-dimensional eigenvalue Λ is of order $O(\alpha^2)$ and the number of oscillations in transverse displacement is of order α (this will be discussed later), and therefore the terms in square brackets in equation (8) are of the same order of magnitude as the largest term outside the brackets. This suggests that the leading approximation to equation (8) can be

obtained by setting $\varepsilon = 0$, i.e.,

$$v'''' + 2\alpha^2 v'''' + (\alpha^4 - \Lambda)v'' + \Lambda v\alpha^2 = 0. \tag{11}$$

This equation with boundary conditions

$$v = v' = v'''' + 2\alpha^2 v'' = 0 \quad \text{at } \bar{s} = 0, 1 \tag{12}$$

gives a leading-order approximation Λ_0 to the non-dimensional eigenvalue Λ,

$$\Lambda = \Lambda_0 + O(\varepsilon).$$

Note that the validity of the equation (11) for large α is limited by the condition $h/R \ll 1$.

Equation (11) is a familiar equation of inextensional (or flexural) in-plane vibration of a ring or portion of a ring [23]. A feature of this equation is that it does not explicitly depend on the beam slenderness parameter (in fact, the slenderness parameter ε enters only the non-dimensional eigenvalue Λ), which suggests that the slenderness parameter of helices and beams with larger opening angle affects only the scaling of natural frequencies. Numerical results show that the inextensional approximation (11, 12) provides sufficient accuracy (up to few per cent) for the non-dimensional eigenvalue of beams with a thickness to length ratio of up to 0·1.

3.2. APPROXIMATION FOR SMALL OPENING ANGLE

In this section, we derive analytical approximations for the non-dimensional eigenvalue of the lower modes using Rayleigh's principle. In doing so, we take advantage of the fact that, for the range of opening angle studied in the present paper, a sufficiently accurate approximation for the non-dimensional eigenvalue may be obtained by assuming that the vibrations are inextensional.

3.2.1. *Modes antisymmetric in v*

An approximation for non-dimensional eigenvalue can be obtained from Rayleigh's principle provided that a reasonable approximation for mode shape is known. We assume that the shape of the transverse displacements of a curved beam is little affected by curvature and therefore can be approximated by that at curvature approaching zero. In the case of antisymmetric modes, the transverse displacements of a straight beam can be taken as an approximation for transverse displacements of a corresponding mode of a curved beam

$$v = a\left\{\cos\frac{\beta}{2}\sinh\left[\beta\left(\bar{s} - \frac{1}{2}\right)\right] - \cosh\frac{\beta}{2}\sin\left[\beta\left(\bar{s} - \frac{1}{2}\right)\right]\right\}, \tag{13}$$

where $\beta = \Lambda^{1/4}|_{\alpha=0}$. In order to satisfy the boundary conditions (6) we require

$$\cos\frac{\beta}{2}\sinh\frac{\beta}{2} - \cosh\frac{\beta}{2}\sin\frac{\beta}{2} = 0. \tag{14}$$

With reasonable accuracy the roots of equation (14) are given by $\beta \approx \pi/2 + 2\pi n$, where n is the mode number and $n = 1$ corresponds to the lowest antisymmetric mode.

The expression for tangential displacements u can be obtained by satisfying the condition

$$u' - \alpha v = 0, \tag{15}$$

that the centreline of the beam is unextended. From equation (15) and the boundary condition (5) we have

$$u = \alpha\int_0^{\bar{s}} v\,\mathrm{d}\bar{s} = \frac{a\alpha}{\beta}\left\{\cos\frac{\beta}{2}\cosh\left[\beta\left(\bar{s}-\frac{1}{2}\right)\right] + \cosh\frac{\beta}{2}\cos\left[\beta\left(\bar{s}-\frac{1}{2}\right)\right] - 2\cos\frac{\beta}{2}\cosh\frac{\beta}{2}\right\}. \tag{16}$$

By Rayleigh's principle, $T = W$, where W and T are strain (bending) and kinetic energies. The expressions for these are given by

$$W = \frac{Ebh^3}{24l^3}\int_0^1 [(v' + \alpha u)']^2\,\mathrm{d}\bar{s}, \tag{17}$$

$$T = \frac{\omega^2\rho bhl}{2}\int_0^1 [u^2 + v^2]\,\mathrm{d}\bar{s}, \tag{18}$$

where b is the width of the cross-section. Substituting the expressions for displacements (13, 16) into the expressions for strain and kinetic energies (17, 18) and using (14) yield

$$W = \frac{a^2Ebh^3}{48\beta l^3}\left\{(\beta^2+\alpha^2)^2(\sinh\beta-\beta)\cos^2\frac{\beta}{2} - (\beta^2-\alpha^2)^2(\sin\beta-\beta)\cosh^2\frac{\beta}{2}\right\}, \tag{19}$$

$$T = \frac{a^2\omega^2\rho bhl}{4\beta}\left\{\left(\frac{\alpha}{\beta}\right)^2\left[-10\cos\frac{\beta}{2}\cosh\frac{\beta}{2}\left(\cosh\frac{\beta}{2}\sin\frac{\beta}{2} + \cos\frac{\beta}{2}\sinh\frac{\beta}{2}\right)\right.\right.$$
$$\left.\left. + \beta\left(\cos^2\frac{\beta}{2} + \cosh^2\frac{\beta}{2}\right) + 8\beta\cos^2\frac{\beta}{2}\cosh^2\frac{\beta}{2}\right] + \beta\left(\cosh^2\frac{\beta}{2} - \cos^2\frac{\beta}{2}\right)\right\}. \tag{20}$$

An expression for the non-dimensional eigenvalue Λ can then be obtained from Rayleigh's principle as

$$\Lambda = \left\{(\beta^2+\alpha^2)^2(\sinh\beta-\beta)\cos^2\frac{\beta}{2} - (\beta^2-\alpha^2)^2(\sin\beta-\beta)\cosh^2\frac{\beta}{2}\right\}$$
$$\times\left\{\left(\frac{\alpha}{\beta}\right)^2\left[-10\cos\frac{\beta}{2}\cosh\frac{\beta}{2}\left(\cosh\frac{\beta}{2}\sin\frac{\beta}{2}+\cos\frac{\beta}{2}\sinh\frac{\beta}{2}\right)\right.\right.$$
$$\left.\left.+\beta\left(\cos^2\frac{\beta}{2}+\cosh^2\frac{\beta}{2}\right)+8\beta\cos^2\frac{\beta}{2}\cosh^2\frac{\beta}{2}\right]+\beta\left(\cosh^2\frac{\beta}{2}-\cos^2\frac{\beta}{2}\right)\right\}^{-1}. \tag{21}$$

From expressions (19, 20), one can see that while the integral in the expression for kinetic energy increases quadratically in α, the strain energy is fourth power of α and is expected to have a minimum. The value α_* that yields a minimum strain energy can be calculated from the condition $\partial W/\partial\alpha = 0$ and is given by

$$\alpha_*^2 = \beta^2\frac{(\beta-\sin\beta)\cosh^2(\beta/2)+(\beta-\sinh\beta)\cos^2(\beta/2)}{(\beta-\sin\beta)\cosh^2(\beta/2)-(\beta-\sinh\beta)\cos^2(\beta/2)}. \tag{22}$$

It can be seen that the value of opening angle that delivers the minimum to the strain energy is a function only of non-dimensional eigenvalue of the corresponding mode of the straight beam. The structure of this dependence becomes more apparent when considering larger values of β. Equation (22) can then be approximated by $\alpha_* \approx \beta \approx \pi/2 + 2\pi n$ and it can be seen that the minima of strain (bending) energy for consecutive antisymmetric modes are spaced 2π apart.

Because the integral in the expression for kinetic energy increases with increasing opening angle of the beam, the position of the minimum of the non-dimensional eigenvalue Λ is shifted a little toward larger opening angle compared to the position of minimum of strain energy. For example, for the lowest antisymmetric mode the minimum of strain energy occurs at $\alpha^* = 2{\cdot}16\pi$, while the minimum of the non-dimensional eigenvalue Λ occurs at $\alpha^* = 2{\cdot}43\pi$.

3.2.2. *Modes symmetric in v*

In the case of the modes symmetric in v, the approximation for transverse displacements can be obtained from equation (11) in the limit $\alpha \to 0$ and is given by

$$v = a\left\{\sinh\frac{\beta}{2}\cos\left[\beta\left(\bar{s}-\frac{1}{2}\right)\right]+\sin\frac{\beta}{2}\cosh\left[\beta\left(\bar{s}-\frac{1}{2}\right)\right]\right.$$
$$\left.-\cosh\frac{\beta}{2}\sin\frac{\beta}{2}-\cos\frac{\beta}{2}\sinh\frac{\beta}{2}\right\}. \tag{23}$$

The boundary conditions (6) are satisfied by requiring

$$\cosh\frac{\beta}{2}\sin\frac{\beta}{2}+\cos\frac{\beta}{2}\sinh\frac{\beta}{2}-\frac{4}{\beta}\sin\frac{\beta}{2}\sinh\frac{\beta}{2}=0. \tag{24}$$

The expression for tangential displacements u satisfying the boundary condition (5) and the conditions that the vibrations are inextensional (15) is given by

$$u=\alpha\int_0^{\bar{s}} v\,\mathrm{d}\bar{s}=\frac{a\alpha}{\beta}\left\{\sin\frac{\beta}{2}\sinh\left[\beta\left(\bar{s}-\frac{1}{2}\right)\right]\right.$$
$$\left.+\sinh\frac{\beta}{2}\sin\left[\beta\left(\bar{s}-\frac{1}{2}\right)\right]+2\sin\frac{\beta}{2}\sinh\frac{\beta}{2}(1-2\bar{s})\right\}. \tag{25}$$

By substituting the expressions for displacements into the expressions for potential and kinetic energies (17, 18) and using Rayleigh's principle gives, for the non-dimensional eigenvalue Λ,

$$\Lambda=\left\{(\beta^2+\alpha^2)^2(\sinh\beta+\beta)\sin^2\frac{\beta}{2}+(\beta^2-\alpha^2)^2(\sin\beta+\beta)\sinh^2\frac{\beta}{2}\right.$$
$$-\frac{16}{\beta}(\beta^4+\alpha^4)\sin^2\frac{\beta}{2}\sinh^2\frac{\beta}{2}\Bigg\}\left\{\left(\frac{\alpha}{\beta}\right)^2\left[\beta\left(\sinh^2\frac{\beta}{2}-\sin^2\frac{\beta}{2}\right)\right.\right.$$
$$\left.-10\sin\frac{\beta}{2}\sinh\frac{\beta}{2}\left(\cosh\frac{\beta}{2}\sin\frac{\beta}{2}-\cos\frac{\beta}{2}\sinh\frac{\beta}{2}\right)+\frac{8\beta}{3}\sin^2\frac{\beta}{2}\sinh^2\frac{\beta}{2}\right]$$
$$\left.+\beta\left(\sinh^2\frac{\beta}{2}+\sin^2\frac{\beta}{2}\right)-\frac{8}{\beta}\sin^2\frac{\beta}{2}\sinh^2\frac{\beta}{2}\right\}^{-1}, \tag{26}$$

where the allowed β values are the roots of equation (24).

The behaviour of the strain and kinetic energy, and as a result the behaviour of non-dimensional eigenvalue, with increasing opening angle, is similar to that of antisymmetric modes considered in the preceding section. In the case of symmetric modes, the value of opening angle that provides the minimum in the strain energy is given by

$$\alpha_*^2=\beta^2\,\frac{(\beta+\sin\beta)\sinh^2\beta/2-(\beta+\sinh\beta)\sin^2\beta/2}{(\beta+\sin\beta)\sinh^2\beta/2+(\beta+\sinh\beta)\sin^2\beta/2-(16/\beta)\sin^2\beta/2\sinh^2\beta/2}. \tag{27}$$

For larger values of β we have $\alpha^* \approx \beta \approx 2\pi n + 3\pi/2$. One can see that, in the same manner as in the case of antisymmetric modes, the minima of the non-dimensional eigenvalue for consecutive symmetric modes are spaced 2π apart and that they lag behind the minima of the antisymmetric modes by π. The minima of the

non-dimensional eigenvalue Λ are again shifted towards larger values of opening angle compared to the minima of strain energy.

3.3. APPROXIMATION FOR LARGE OPENING ANGLE

In this section, we obtain approximations for the non-dimensional eigenvalue and mode shape at large opening angle on the basis of asymptotic analysis of the equation of inextensional vibration (11). In the following analysis, a parameter $\delta = \sqrt{\Lambda}/\alpha^2$ is considered to be small and it is assumed that $\delta = O(1/\alpha)$.

3.3.1. *Non-dimensional eigenvalues of symmetric modes*

For the modes symmetric in v, the general solution of equation (11) has the form

$$v = c_1 \cos[\beta_1 \alpha(\bar{s} - 1/2)] + c_2 \cos[\beta_2 \alpha(\bar{s} - 1/2)] + c_3 \cos[\beta_3 \alpha(\bar{s} - 1/2)], \quad (28)$$

where β_i are the roots of the equation

$$\beta^2(\beta^2 - 1)^2 = \delta^2(\beta^2 + 1).$$

It is easy to show that

$$\beta_1 = \delta + O(\delta^2), \quad \beta_2 = 1 - \frac{\delta}{\sqrt{2}} + O(\delta^2), \quad \beta_3 = 1 + \frac{\delta}{\sqrt{2}} + O(\delta^2). \quad (29)$$

The non-dimensional eigenvalue Λ can be obtained by substituting expression (28) into the boundary conditions (12) and requiring that the resulting system of equation in c_i has a non-trivial solution. Thus

$$\begin{vmatrix} \cos(\beta_1\alpha/2) & \cos(\beta_2\alpha/2) & \cos(\beta_3\alpha/2) \\ \beta_1 \sin(\beta_1\alpha/2) & \beta_2 \sin(\beta_2\alpha/2) & \beta_3 \sin(\beta_3\alpha/2) \\ \beta_1^3(\beta_1^2 - 2)\sin(\beta_1\alpha/2) & \beta_2^3(\beta_2^2 - 2)\sin(\beta_2\alpha/2) & \beta_3^3(\beta_3^2 - 2)\sin(\beta_3\alpha/2) \end{vmatrix} = 0.$$

Up to order $O(\delta^3)$, this equation can be reduced to

$$-\beta_1 \sin(\beta_1\alpha/2)[\beta_3^3(\beta_3^2 - 2)\sin(\beta_3\alpha/2)\cos(\beta_2\alpha/2)$$

$$-\beta_2^3(\beta_2^2 - 2)\cos(\beta_3\alpha/2)\sin(\beta_2\alpha/2)] = 0.$$

Obviously, this equation has two families of solutions. The first family is given by the equation

$$\sin(\beta_1\alpha/2) = 0$$

the solution of which is

$$\Lambda_k^{\mathrm{I}} = 4\alpha^2(\pi k)^2, \quad k = 1, 2, \ldots \quad (30)$$

The second family is given by the equation

$$\beta_3^3(\beta_3^2-2)\sin(\beta_3\alpha/2)\cos(\beta_2\alpha/2)-\beta_2^3(\beta_2^2-2)\cos(\beta_3\alpha/2)\sin(\beta_2\alpha/2)=0,$$

which can be rewritten, up to the order $O(\delta^2)$, as

$$\sin\left[\frac{\alpha(\beta_3-\beta_2)}{2}\right]=\frac{\alpha(\beta_3-\beta_2)}{2}\frac{\sin\alpha}{\alpha}.$$

Given that $\sin\alpha/\alpha=O(\delta)$, this equation can be solved asymptotically for small δ. Thus, to $O(k\delta^2)$, we have

$$(\beta_3-\beta_2)\alpha/2=k\pi\left[1-(-1)^k\frac{\sin\alpha}{\alpha}\right],$$

and therefore the non-dimensional eigenvalue for the second family is given by

$$\Lambda_k^{\mathrm{II}}=2k^2\pi^2\alpha[\alpha-(-1)^k 2\sin\alpha]+O(1),\quad k=1,2,\ldots \tag{31}$$

3.3.2. *Non-dimensional eigenvalues of antisymmetric modes*

In a similar manner, an approximation for non-dimensional eigenvalue can be derived for antisymmetric modes. In this case, the general solution has the form

$$v=c_1\sin[\beta_1\alpha(\bar{s}-1/2)]+c_2\sin[\beta_2\alpha(\bar{s}-1/2)]+c_3\sin[\beta_3\alpha(\bar{s}-1/2)] \tag{32}$$

and the non-dimensional eigenvalue is defined by the equation

$$\begin{vmatrix} \cos(\beta_1\alpha/2) & \cos(\beta_2\alpha/2) & \cos(\beta_3\alpha/2) \\ \beta_1\sin(\beta_1\alpha/2) & \beta_2\sin(\beta_2\alpha/2) & \beta_3\sin(\beta_3\alpha/2) \\ \beta_1^3(\beta_1^2-2)\sin(\beta_1\alpha/2) & \beta_2^3(\beta_2^2-2)\sin(\beta_2\alpha/2) & \beta_3^3(\beta_3^2-2)\sin(\beta_3\alpha/2) \end{vmatrix}=0.$$

which can be written up to $O(\delta^3)$ as

$$-\beta_1\cos(\beta_1\alpha/2)[\beta_3^3(\beta_3^2-2)\cos(\beta_3\alpha/2)\sin(\beta_2\alpha/2)$$

$$-\beta_2^3(\beta_2^2-2)\sin(\beta_3\alpha/2)\cos(\beta_2\alpha/2)]=0.$$

The two families of solutions for the non-dimensional eigenvalue are given by

$$\cos(\beta_1\alpha/2)=0$$

TABLE 1

Non-dimensional eigenvalue of the two families of approximations

	Symmetric		Antisymmetric	
k	Λ_k^{I}	Λ_k^{II}	Λ_k^{I}	Λ_k^{II}
1	$4(\pi\alpha)^2$	$2(\pi\alpha)^2$	$(\pi\alpha)^2$	$2(\pi\alpha)^2$
2	$16(\pi\alpha)^2$	$8(\pi\alpha)^2$	$9(\pi\alpha)^2$	$8(\pi\alpha)^2$
3	$36(\pi\alpha)^2$	$18(\pi\alpha)^2$	$25(\pi\alpha)^2$	$18(\pi\alpha)^2$

TABLE 2

Approximations in ascending order of frequency

Symmetric	Λ_1^{II},	Λ_1^{I},	Λ_2^{II},	Λ_2^{I},	Λ_3^{II},	Λ_3^{I}
Antisymmetric	Λ_1^{I},	Λ_1^{II},	Λ_2^{II},	Λ_2^{I},	Λ_3^{II},	Λ_3^{I}

and

$$\beta_3^3(\beta_3^2 - 2)\cos(\beta_3\alpha/2)\sin(\beta_2\alpha/2) - \beta_2^3(\beta_2^2 - 2)\sin(\beta_3\alpha/2)\cos(\beta_2\alpha/2)$$

$$= \sin\left[\frac{\alpha(\beta_3 - \beta_2)}{2}\right] - \frac{\alpha(\beta_3 - \beta_2)}{2}\,\frac{\sin\alpha}{\alpha} + O(\delta^2) = 0.$$

The non-dimensional eigenvalue corresponding to the first family is given by

$$\Lambda_k^{\mathrm{I}} = (\pi\alpha)^2(2k - 1)^2, \quad k = 1, 2, \ldots, \tag{33}$$

while the non-dimensional eigenvalue for the second family is given by

$$\Lambda_k^{\mathrm{II}} = 2k^2\pi^2\alpha[\alpha + (-1)^k 2\sin\alpha] + O(1), \quad k = 1, 2, \ldots \tag{34}$$

The values of non-dimensional eigenvalue for the three lowest approximations at large α are shown in Table 1. It can be seen that the non-dimensional eigenvalues as functions of opening angle for approximation of a given symmetry do not intersect and it is therefore possible to arrange them in ascending order of frequency (see Table 2). This order is different for symmetric and antisymmetric modes, and it will be seen later that it defines the order in which the modes of a curved beam take one or another type of vibrational behaviour at large opening angle. While this order is actually well defined, it has the appearance of being almost random.

3.3.3. *Mode shapes at large opening angle*

In this section, we shall obtain the approximations for the eigenfunctions and show that they have a specific structure depending on the value of the non-dimensional eigenvalue.

In order to obtain the expressions for eigenfunctions up to a multiplying constant, we can set one of the coefficients c_i in expressions (28, 32) equal to 1 and estimate the remaining coefficients from boundary conditions. If we set $c_3 = 1$, then

$$c_1 = \frac{-\beta_2 f\left(\frac{\beta_3\alpha}{2}\right) g\left(\frac{\beta_2\alpha}{2}\right) + \beta_3 f\left(\frac{\beta_2\alpha}{2}\right) g\left(\frac{\beta_3\alpha}{2}\right)}{\beta_2 f\left(\frac{\beta_1\alpha}{2}\right) g\left(\frac{\beta_2\alpha}{2}\right) - \beta_1 f\left(\frac{\beta_2\alpha}{2}\right) g\left(\frac{\beta_1\alpha}{2}\right)},$$

$$c_2 = \frac{-\beta_3 f\left(\frac{\beta_1\alpha}{2}\right) g\left(\frac{\beta_3\alpha}{2}\right) + \beta_1 f\left(\frac{\beta_3\alpha}{2}\right) g\left(\frac{\beta_1\alpha}{2}\right)}{\beta_2 f\left(\frac{\beta_1\alpha}{2}\right) g\left(\frac{\beta_2\alpha}{2}\right) - \beta_1 f\left(\frac{\beta_2\alpha}{2}\right) g\left(\frac{\beta_1\alpha}{2}\right)},$$

where

$$f \equiv \begin{cases} \cos & \text{for symmetric modes,} \\ \sin & \text{for antisymmetric modes,} \end{cases}$$

$$g \equiv \begin{cases} \sin & \text{for symmetric modes,} \\ \cos & \text{for antisymmetric modes.} \end{cases}$$

Firstly, consider the non-dimensional eigenvalue given by the second family of solutions (31) and (34). Substituting these expressions into equation (29), and the latter into the above expressions for c_1 and c_2, and taking limit $\alpha \to \infty$ yield

$$c_1 \to 0, \quad c_2 \to (-1)^{k+1},$$

where k is the mode index defined by equations (31, 34). Therefore, the form of normal displacements at large opening angle is, up to a constant,

$$v \approx \begin{cases} \cos[\alpha(\bar{s} - 1/2)] \cos[k\pi(\bar{s} - 1/2)] & \text{for odd } k, \\ \sin[\alpha(\bar{s} - 1/2)] \sin[k\pi(\bar{s} - 1/2)] & \text{for even } k \end{cases}$$

for symmetric modes, and

$$v \approx \begin{cases} \sin[\alpha(\bar{s} - 1/2)] \cos[k\pi(\bar{s} - 1/2)] & \text{for odd } k, \\ \cos[\alpha(\bar{s} - 1/2)] \sin[k\pi(\bar{s} - 1/2)] & \text{for even } k \end{cases}$$

for antisymmetric modes. We can see that the normal displacements in this case are highly oscillatory functions with spatial frequency of oscillation proportional to the opening angle, modulated by a slowly varying function with frequency proportional to the mode index k in the particular family of approximations. The tangential displacements in this case have similar structure and are of the same order of magnitude as the transverse displacements.

When the non-dimensional eigenvalue takes the values from the first family of solutions (30) and (33), the structure of the normal displacements is more complicated and generally all three terms in expressions (28, 32) play significant roles. In this case, it is convenient to consider the structure of the tangential displacements, which is more clearly defined. The tangential displacements have the form

$$u = b_1 g\,[\beta_1\alpha(\bar{s} - 1/2)] + b_2 g\,[\beta_2\alpha(\bar{s} - 1/2)] + b_3 g[\beta_3\alpha(\bar{s} - 1/2)] + \text{const}, \quad (35)$$

where

$$b_j = \frac{c_j}{\beta_j}, \quad j = 1, 2, 3. \quad (36)$$

It is convenient in this case to set $c_1 = 1$, then we have the following expressions for the remaining coefficients:

$$c_2 = \frac{-\beta_3 f\left(\frac{\beta_3\alpha}{2}\right) g\left(\frac{\beta_1\alpha}{2}\right) + \beta_1 f\left(\frac{\beta_1\alpha}{2}\right) g\left(\frac{\beta_3\alpha}{2}\right)}{\beta_3 f\left(\frac{\beta_3\alpha}{2}\right) g\left(\frac{\beta_2\alpha}{2}\right) - \beta_2 f\left(\frac{\beta_2\alpha}{2}\right) g\left(\frac{\beta_3\alpha}{2}\right)}, \quad (37)$$

$$c_3 = \frac{-\beta_1 f\left(\frac{\beta_1\alpha}{2}\right) g\left(\frac{\beta_2\alpha}{2}\right) + \beta_2 f\left(\frac{\beta_2\alpha}{2}\right) g\left(\frac{\beta_1\alpha}{2}\right)}{\beta_3 f\left(\frac{\beta_3\alpha}{2}\right) g\left(\frac{\beta_2\alpha}{2}\right) - \beta_2 f\left(\frac{\beta_2\alpha}{2}\right) g\left(\frac{\beta_3\alpha}{2}\right)}. \quad (38)$$

By substituting the expressions for Λ from equations (30, 33) into equation (29) and the latter into equations (37, 38) and (36), it is easy to show that

$$b_1 = O(\alpha), \quad b_2 = O(1), \quad b_3 = O(1) \quad \text{as } \alpha \to \infty.$$

The shape of tangential displacements, up to the leading order, is given by

$$u \approx \begin{cases} \alpha \sin\,[2k\pi(\bar{s} - 1/2)] & \text{for symmetric modes,} \\ \alpha \cos\,[(2k-1)\pi(\bar{s} - 1/2)] & \text{for antisymmetric modes,} \end{cases}$$

where $k = 1, 2, \ldots$ It can be seen that the leading-order part of the tangential displacements is a slowly varying function with a number of half-waves

proportional to the mode index k in a corresponding family of approximations. The transverse displacements in this case are of smaller order of magnitude than the tangential ones

$$v = O(1).$$

It can be seen that the major difference in the structure of mode shape for the two families of approximations, in terms of tangential displacements, is that in the case of the first family the tangential displacements are, to the leading order, slowly varying functions, with number of oscillations proportional to the mode index in its family, while in the case of the second family the tangential displacements are highly oscillatory functions with number of oscillations proportional to the value of opening angle. In what follows, we designate these as type I and type II modes, respectively.

Finally, it should be noted that the results with respect to vibrational behaviour at larger opening angle can be obtained, in less rigorous but perhaps more illuminating way, directly from Rayleigh's principle, which can be written in terms of tangential displacements as

$$\Lambda = \min_{u} \frac{\int_0^1 (u'''/\alpha + \alpha u')^2 \, \mathrm{d}\bar{s}}{\int_0^1 (u^2 + u'^3/\alpha^2) \, \mathrm{d}\bar{s}}. \tag{39}$$

There are two possibilities to consider here in the limit of large opening angle. The first is to assume that the tangential displacements are relatively slowly varying functions, with number of half-waves of an order less than α. Then, in the limit of large opening angle, equation (39) can be considerably simplified to

$$\Lambda = \min_{u} \frac{\int_0^1 (\alpha u')^2 \, \mathrm{d}\bar{s}}{\int_0^1 u^2 \, \mathrm{d}\bar{s}} \quad \text{as } \alpha \to \infty$$

which is equivalent to the equation

$$\alpha^2 u'' = \Lambda u.$$

Obviously, this equation with boundary conditions $u(0) = u(1) = 0$ produces the solution for the non-dimensional eigenvalue of the first family.

Another possibility is to suggest that all terms in the integrands of equation (39) are of the same order, which means that the number of half-waves in u is of order α. It can be shown that with this assumption equation (39), solved in the limit of large opening angle, will produce the solution for the non-dimensional eigenvalue of the second family.

4. NUMERICAL RESULTS

The non-dimensional eigenvalue of the lowest symmetric mode of a uniformly curved beam is shown in Figure 1. Broken lines represent the numerical solution for

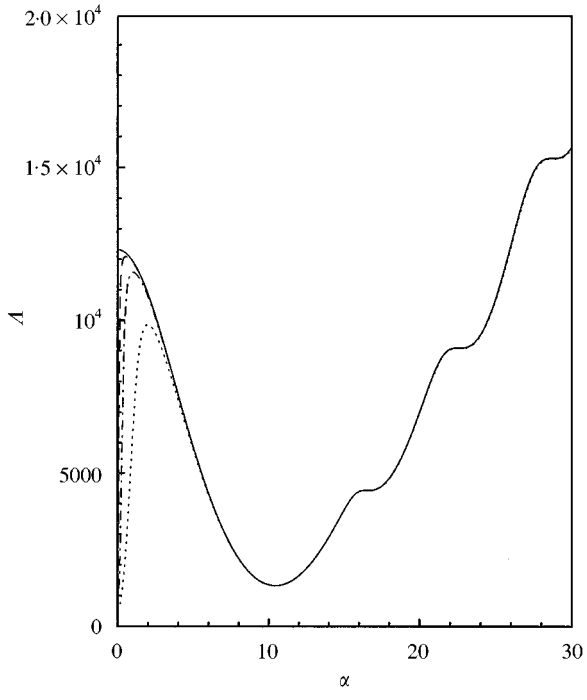

Figure 1. Non-dimensional eigenvalue Λ as a function of opening angle α for lowest symmetrical mode. The length of the beam remains constant and the curvature is increased. Inextensional approximation is shown by solid line, broken lines show the numerical solution for different values of ε: - - - $\varepsilon = 10^{-6}$, -·-·- $\varepsilon = 10^{-5}$, ···· $\varepsilon = 10^{-4}$.

different values of the slenderness parameter ε, calculated using equations (1, 2). The solid line shows the inextensional solution calculated using equations (11, 12). We can see that the inextensional solution represents an accurate approximation everywhere outside the region of initial small-curvature transformation of the modes.

In Figure 2, we have plotted the numerical inextensional solution and small opening angle analytic approximations for the non-dimensional eigenvalue of the lowest antisymmetric and symmetric modes versus opening angle. We can see that the analytic approximation provides an accurate description of the region of decrease and subsequent rise of the non-dimensional eigenvalue and also gives an accurate prediction of the position of its minimum. However, the vibrational behaviour for larger opening angle cannot be predicted by this approximation. This is not surprising because the assumption that the mode shape remains without change becomes invalid at that stage.

In Figures 3 and 4, the non-dimensional eigenvalues of the lowest three symmetric and antisymmetric modes are shown together with large opening angle analytic approximations. It can be seen that the analytic approximations give an accurate prediction of non-dimensional eigenvalues for large values of opening

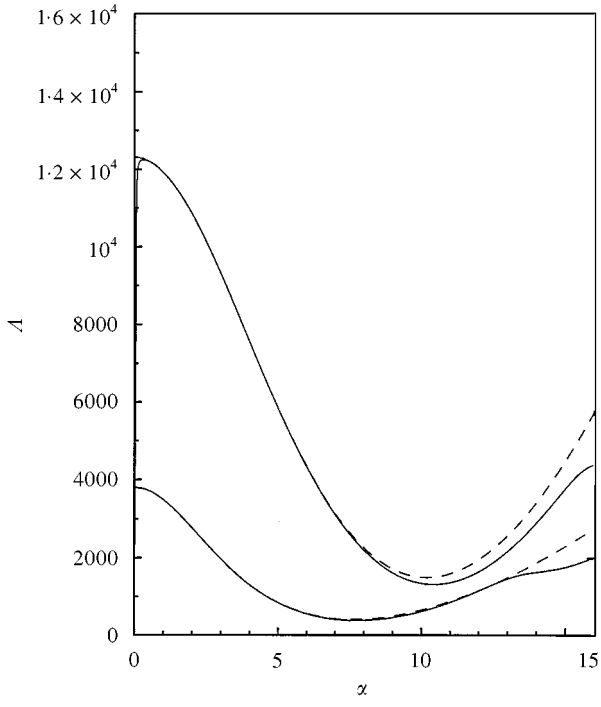

Figure 2. Non-dimensional eigenvalue as a function of opening angle for the lowest antisymmetric and symmetric modes (lower non-dimensional eigenvalue corresponds to antisymmetric mode). Inextensional solution is shown by solid line, while analytical approximations are shown by dashed lines.

angle. The analytic approximations for the lowest two symmetric and antisymmetric modes are almost indistinguishable from the exact numerical solution for a wide range of the opening angle. It is interesting to note that in the case of symmetric modes, the second mode belongs to the first type of vibrational behaviour at large opening angle, while the lowest and the third modes belong to the second type. This is also clearly demonstrated in Figure 5, where the displacements of the three lowest symmetric modes are shown at large value of opening angle. In the case of antisymmetric modes the order is different. The lowest mode belongs to the first type of vibrational behaviour, while the next two modes belong to the second type (see also Figure 6). It appears that the order of the modes (when arranged in ascending order of frequency) in the analytic approximation of a particular type of symmetry defines the order in which the modes of a curved beam of the same type of symmetry take one or another type of vibrational behaviour at large opening angle.

5. PHYSICAL INTERPRETATION

Because the vibrational phenomena discussed above are complex, it is important to be able to describe them in simple terms and to give physical reasons for their appearance and behaviour. Specifically, a physical explanation is desirable for (1)

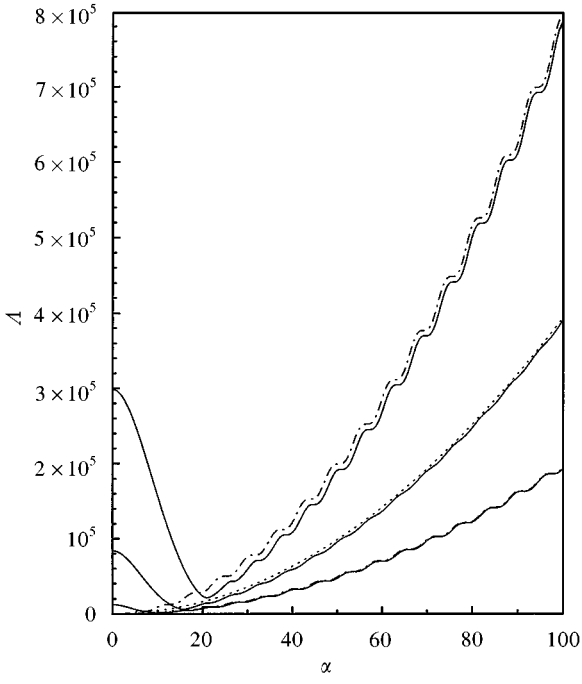

Figure 3. Numerical solution (solid lines) and large opening angle analytic approximations for non-dimensional eigenvalue of symmetric modes. The analytic approximations of the first family are shown by dotted lines, while the approximations of the second family are shown by dashed-dotted lines (note that the approximation is virtually indistinguishable from the non-dimensional eigenvalue of the lowest mode).

the decrease in mode frequency to a minimum value for moderate curvature, and the relationship between the mode number and the curvature for which this minimum occurs, and (2) the mode behaviour at very high values of curvature. We approach these in turn.

As discussed in our earlier papers [12, 14], the transverse modes of a straight beam are, of course, inextensional to first order. When the beam is curved, those modes that are antisymmetric about the centre of the beam remain inextensional, while symmetric modes have an extensional component that is proportional to the non-dimensional beam curvature (or opening angle) α. The frequencies of antisymmetric modes are therefore independent of curvature, to a first approximation, and need concern us no further. The frequencies of symmetric modes, on the other hand, rise sharply with increasing curvature. It then becomes energetically favourable, in the sense of a variational principle, to modify each symmetric mode function by adding to it a proportion of the next-higher symmetric mode function in such a way that the extensions have opposite signs and cancel as discussed in reference [14]. The resulting variational energy, and thus the frequency, lies between those of the two modes that have been combined and, the new mode being inextensional, suffers no further frequency change as the curvature is increased. It is these modified modes that formed the starting point for our present analysis, for these transformations all occur for $\alpha \ll 1$.

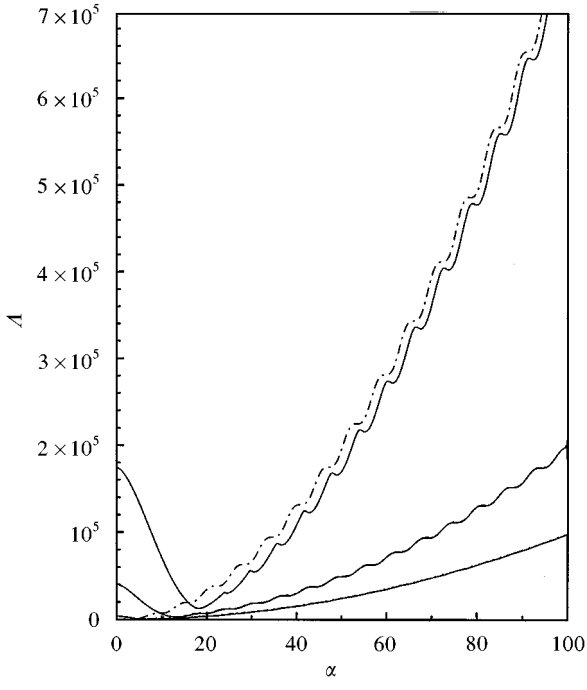

Figure 4. Numerical solution (solid lines) and large opening angle analytic approximations for non-dimensional eigenvalue of antisymmetric modes. The analytic approximations of the first family are shown by dotted lines (the approximation is virtually indistinguishable from the non-dimensional eigenvalue of the lowest mode), while the approximations of the second family are shown by dashed-dotted lines (second and third modes).

For values of the opening angle α small compared with 2π, the beam displacements are predominantly transverse, so that longitudinal kinetic energy can be ignored when calculating the frequency by means of Rayleigh's principle. As the opening angle is increased, however, longitudinal motion becomes more and more important, if we assume the transverse form of the beam modes to remain unaltered. This is because a simple expansion of one turn of a helix is necessarily coupled to a longitudinal motion that is 2π times as large.

As the opening angle α is increased, a situation is reached in which the number of turns in the helix is equal to the number of full wavelengths in the mode function under consideration. At this point, each turn of the helix suffers a transverse displacement of the form $\sin\phi$, where ϕ is the azimuthal angle around the helix, and to this is coupled a longitudinal displacement $\cos\phi$, resulting in a simple sideways motion of the whole helical turn with no elastic distortion whatever. The whole helix, except near its clamped ends, suffers a similar displacement. This is the situation when $\alpha \approx 2n\pi$ for antisymmetric modes and when $\alpha \approx (2n+1)\pi$ for symmetric modes, where n is the mode number of the modified modes discussed above. Almost the only elastic distortion in this case occurs at the clamped ends of the helix, and the mode concerned has a frequency minimum near this value of α. When the curvature matching condition is not exactly met, then the displacement

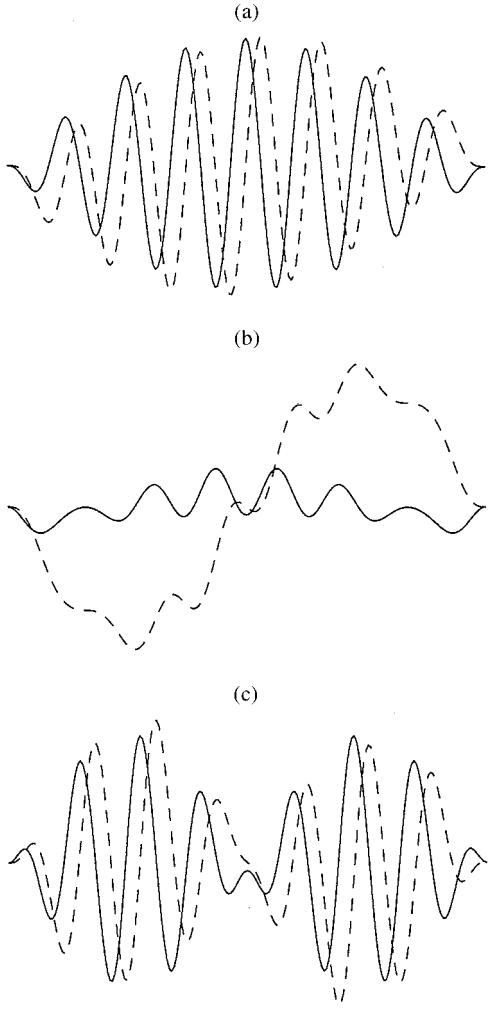

Figure 5. Displacements of the three lowest symmetric modes at $\alpha = 50$. Transverse displacements are shown by solid lines, while tangential displacements are shown by dashed lines: (a) first mode, (b) second mode, (c) third mode.

of the helix is to the form of a super-helix with about $n - \alpha/2\pi$ turns, the sign of this quantity determining whether the super-helix winds in the same or the opposite sense to the base helix. The elastic energy associated with this super-helical distortion ensures that the frequency rises quadratically with $\alpha - 2\pi n$ in the immediate vicinity of the minimum.

For very large values of α, the analysis of section 3 shows that the transverse displacement v for symmetric modes can be expressed as the sum of three terms as in equation (28). Each term is sinusoidal and has a spatial frequency β_i given by equation (29). Now, from equations (3) and (4), the parameter δ occurring in equation (29) is seen to be simply $\delta = \omega l/c$, where c is the transverse wave speed on the original straight beam. The three terms in v therefore represent transverse

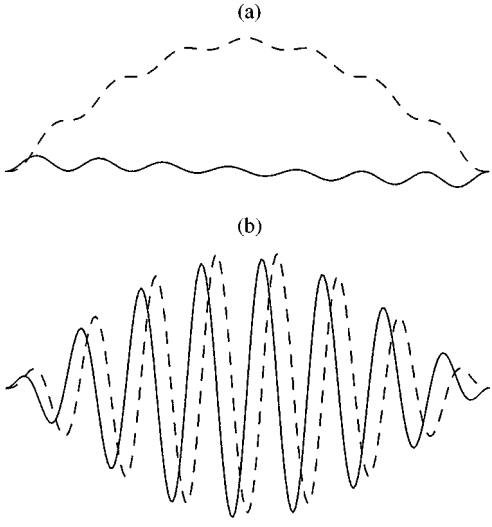

Figure 6. Displacements of the two lowest anti-symmetric modes at $\alpha = 50$. Transverse displacements are shown by solid lines, while tangential displacements are shown by dashed lines: (a) first mode, (b) second mode.

disturbances with respectively n, $(\alpha/2\pi) - (n/\sqrt{2})$ and $(\alpha/2\pi) + (n/\sqrt{2})$ sinusoidal wavelengths along the helical centreline. From our discussion above, on the assumption that $n \ll \alpha$, these represent, in turn, a periodic dilatational motion of the helix, and super-helical distortions of opposite sense. From the discussion in section 3.3.3, there are two types of resulting modes. In modes of type II, the second and third terms dominate and are approximately equal in magnitude, so that the super-helices combine to give a plane-polarized wave-like distortion to the helix, as shown in Figure 7(b). In modes of type I, the first term dominates, and the distortion is a dilatational one, as shown in Figure 7(a). The exact form of these modes depends a little upon whether or not α/π is an integer, as indicated in equations (31, 34), representing an integral number of half-turns on the helix.

The fact that type I and Type II modes have comparable energies is, at first sight, strange. Type II modes clearly have much less elastic distortion energy than do type I modes, but this is compensated for by the very large inertia associated with longitudinal motion in type I modes. Rather more surprising is the fact that, in the large curvature limit, the energies of these two types of modes are locked into a numerical relationship, as shown in Tables 1 and 2.

Viewing the two types of modes macroscopically as vibrations of a helix, rather than microscopically as those of a curved beam, modes of type I might be termed "varicose" and those of type II "sinuous". From a slightly different macroscopic viewpoint, type I modes could be characterized as torsional, with the torsion axis being the axis of the helix, since for these modes tangential displacements are much larger than radial ones. Type II modes could similarly be termed transverse on the macroscopic helix. Note that macroscopic longitudinal modes of the helix derive from out-of-plane modes of the original slightly curved beam, and so are not included in the present analysis.

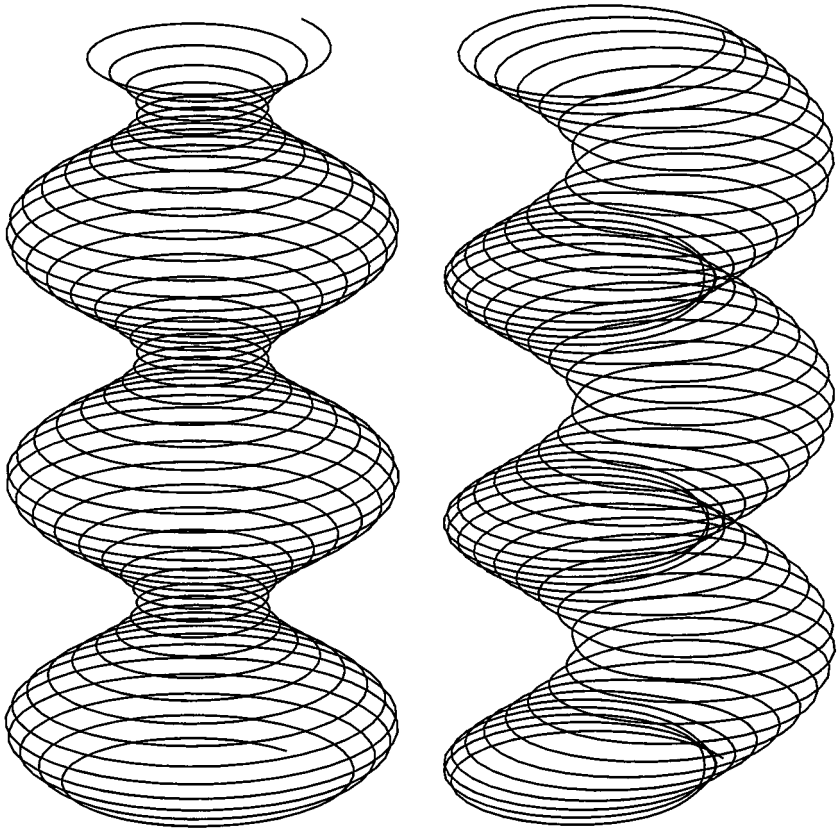

Figure 7. Displacement associated with a typical mode in the region of large α: (a) mode of type I; (b) mode of type II.

6. EXPERIMENTAL VERIFICATION

The predictions of the theory were examined in several experiments. The first two experiments examined the behaviour of the mode frequencies as the opening angle was increased, in one case by simply increasing from zero to a moderately large value the curvature of a beam of constant length, and in the other by progressively reducing the length of a helix of constant curvature. In the final experiment, the vibrational modes of a compact helix were examined and their forms related to the predictions of the theory. While it would have been possible in principle to use a standard instrumented hammer and accelerometer to examine the mode structure, this proved impractical because of the lightness of the helix, and alternative methods were therefore used.

6.1. MODE FREQUENCIES

In each of the first two experiments, the beam was formed from a strip of galvanized steel sheet with thickness 1 mm and width 10 mm. In the first

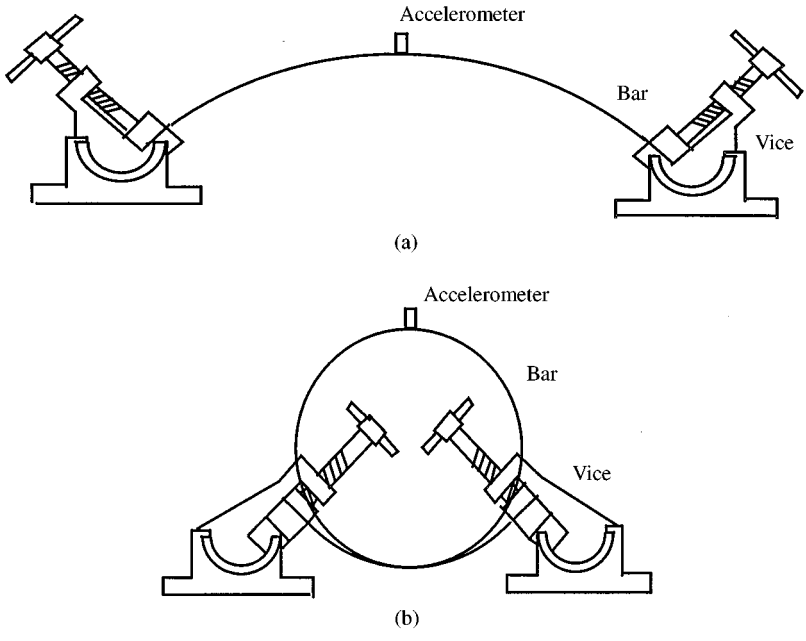

Figure 8. Experimental arrangement for the frequency spectrum measurements of the beam, for small and large curvatures. Note the accelerometer placed in this case in the centre of the beam.

experiment, the length of the beam was 800 mm, and its two ends were clamped in angularly adjustable vices which were in turn clamped to a solid bench as shown in Figure 8. In this way, the curvature of the strip could be varied from zero to a helix of several turns by plastic deformation, so that the opening-angle range $0 \leqslant \alpha \leqslant 25$ could be explored. In the second experiment, a strip of initial length 2400 mm was plastically deformed to a helix of constant radius 48 mm and pitch just a few millimetres greater than the width of the strip. The accuracy of the beam shape was approximately $\pm 3\%$ of its helical radius over its entire length. During the experiment, the opening-angle range $6 \leqslant \alpha \leqslant 50$ was explored by progressively reducing the length of the helix from 2400 to 300 mm by cutting material from one end.

The curved beam or helix was excited into vibration by giving it a sharp tap with a light rod. The position of the tap could be varied to aid in identification of the modes. The vibration was monitored using a sub-miniature Bruel and Kjaer accelerometer, Type 4374, fixed to the surface of the bar with wax. The weight of this accelerometer, the range of which extends to 26 kHz, is only 0·65 g, so that its extra load had negligible effect on the bar vibration. A dual-channel FFT analyzer (ONOSOKKI model CF-350/360 with 100 kHz sampling rate) was then used to collect, process and store the experimental data from the accelerometer.

To reduce measurement uncertainties, 16 measurements were taken for each experimental condition. Each set of data was subjected to a FFT and all 16 sets of results were then averaged. In order to identify symmetric and antisymmetric modes in the frequency spectrum, two sets of measurements with different tapping

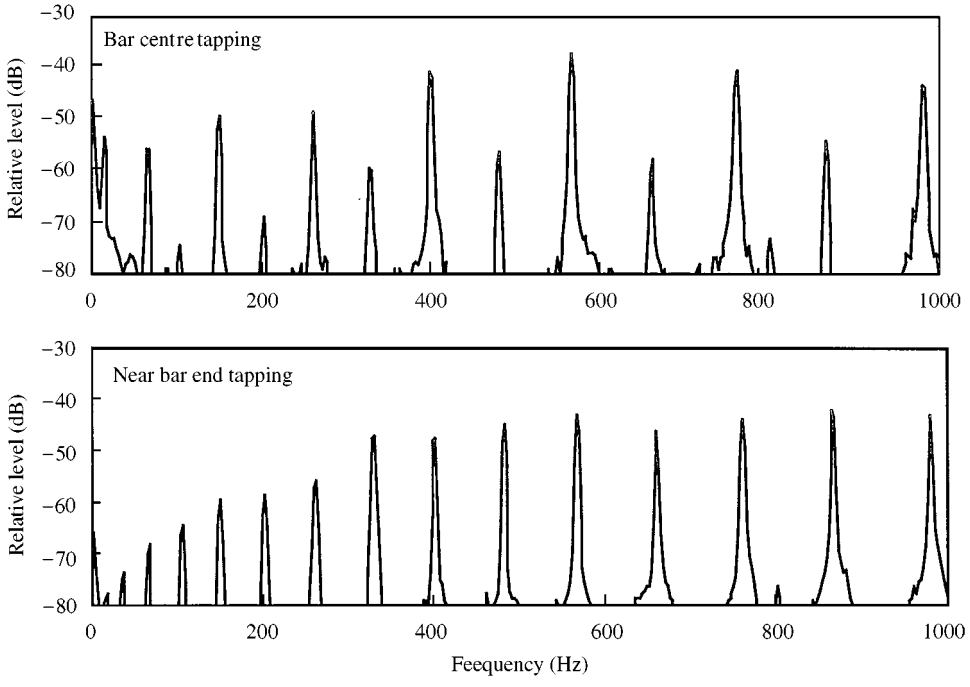

Figure 9. Typical measured vibrational spectra for a curved beam (a) tapped near the mid-point and (b) tapped near one end. In each case, the accelerometer positions were in the centre of the beam. Symmetric and antisymmetric modes are clearly identifiable.

positions were taken. Thus, tapping the bar in the centre excited symmetric modes, while tapping the bar near one of the ends excited all modes nearly equally. Two typical frequency spectra with tapping in the centre and near one of the ends of the bar respectively are shown in Figure 9. For each experiment, four different accelerometer positions were used to help identify modes within these categories. Thus, an accelerometer position about one-quarter of the length from one end of the helix gave maximum response for the second and sixth antisymmetric modes, while a placement at one-eighth of the length accentuated the fourth antisymmetric mode, and so forth. The fact that the accelerometer is sensitive only along its axis ensured identification of axial modes along the helix, which are not included in the theoretical discussion.

Figure 10 shows the measured mode frequencies for the case in which the length of the bar was maintained constant and the curvature varied. Theoretical curves were calculated using equations (1, 2). Since the values of Young's modulus and thickness of the experimental beam were not known to high accuracy, it was impossible to check absolute agreement between measured and calculated frequency. Excellent agreement between theoretical and experimental results is obtained if the parameters of the beam are in the range $5300 \leqslant \sqrt{E/\rho} \leqslant 5400$ m/s, which is consistent with the manufacturer's data. Figure 11 shows the same information for the case in which the curvature was held constant and length varied, thus encompassing a much greater range of the parameter α. Again, the theoretical curves are in good agreement with those in the experiment.

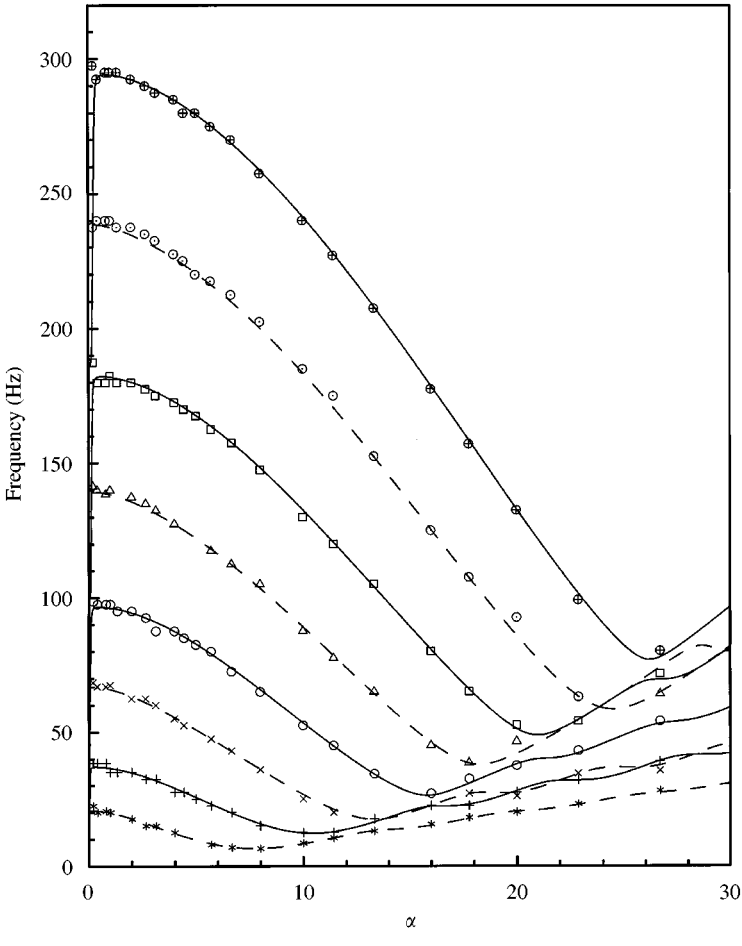

Figure 10. Measured mode frequencies, as functions of beam opening angle, for the case in which the beam length l was kept constant and the curvature varied. Curves show the calculated behaviour (symmetric modes are shown by solid lines, while antisymmetric modes are shown by dashed lines).

6.2. MODE SHAPES

The experiments described above, however, give very limited information about mode shape, and such information is important in view of the predicted existence of modes of two distinct types for large values of the curvature. The final set of experiments aimed to examine this prediction.

Since the mode shapes in question occur only at high values of curvature with $\alpha > 10$, the experiments were carried out on a helix with approximately eight turns ($\alpha \approx 50$). This was made from the same 1 mm steel sheet, and the helix, again 48 mm in radius, was wound with only about 1 mm between turns. Its shape was again maintained by stable plastic distortion of the strip, and was accurate to about ± 1 mm. The helix was clamped as before between the jaws of two heavy vices.

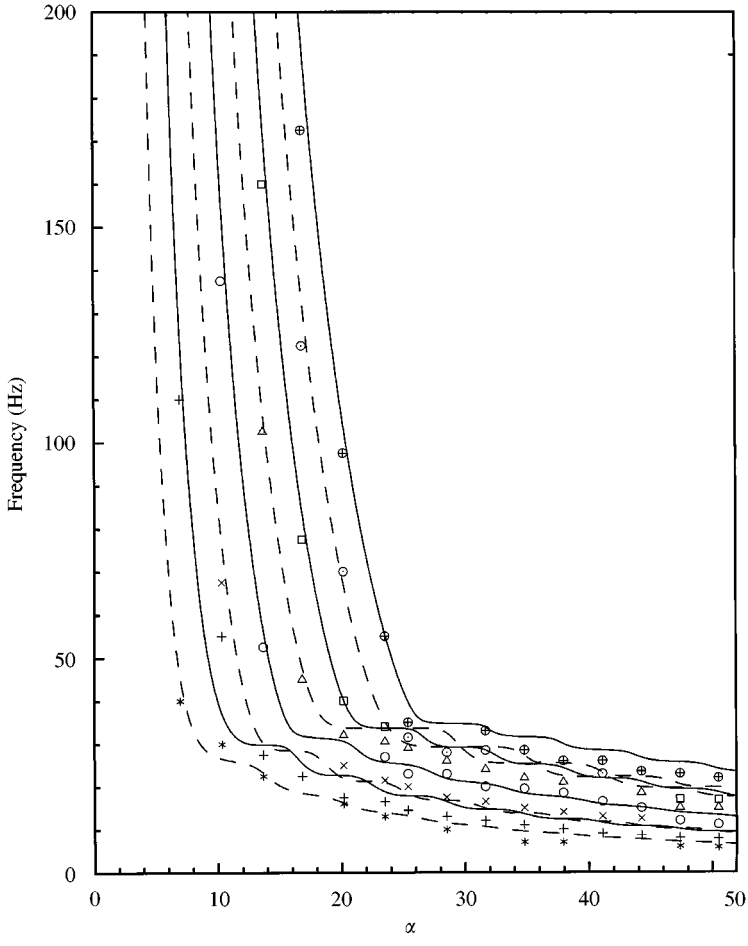

Figure 11. Measured mode frequencies, as functions of beam opening angle, for the case in which the curvature was held constant and the beam length varied (the symbols used to denote the measured frequencies of different modes are as in Figure 10). Full curves show the calculated behaviour (symmetric modes are shown by solid lines).

A preliminary survey of the mode frequencies of the helix was made by tapping it and analysing the signal from an attached accelerometer. The helix was then driven sinusoidally by a shaker mounted only a few millimetres from one of the clamps in such a way as to excite each one of the modes successively for study. With a typical maximum vibrational amplitude of about 1 mm and a mode frequency in the range 5–20 Hz, it was quite simple to discern the shape of the modes by simple visual observation. This was supplemented, however, by stroboscopic illumination, which made the mode structure even more obvious. Finally, the amplitude and phase relations between adjacent helical turns and around individual turns, for both radial and tangential components of the vibration, were examined using a subminiature accelerometer attached in one of two possible orientations with wax. In this way it was very simple to determine the macroscopic shape of each mode for comparison with Figure 7, to verify that these shapes agreed with the

TABLE 3

Experimentally observed mode characteristics

Frequency (Hz)	Mode type	Number of half-wavelengths
5·75	Varicose (I)	1
7·05	Longitudinal	1
7·63	Sinuous (II)	1
7·75	Sinuous (II)	1
11·1	Varicose (I)	2
13·6	Longitudinal	2
14·3	Sinuous (II)	2
16·9	Sinuous (II)	2
22·0	Varicose (I)	3

theoretical predictions for type I and type II modes in relation to both radial and tangential motion, and to classify each mode unambiguously.

The results of these experiments are summarized in Table 3. The third column of the table gives the number of macroscopic half-wavelengths exhibited by the mode. Two longitudinal modes (axial modes on the helix) are included for completeness, but are not relevant to our current study since they derive from out-of-plane modes of the original bent beam, which have not been included in the theory. Omitting these longitudinal modes, it is clear that we have identified both varicose (Type I) and sinuous (type II) modes, and that the frequency sequence of these goes as I,II,II,I,II,II,I,... as predicted by the theory and documented in Table 1. When there are two neighbouring modes of type I, observation shows that they occur as linearly polarized vibrations at approximately 90° to one another, rather than as two super-helical modes. Such a coupling is not unexpected when the effect of the end-conditions is taken into account.

The experiments thus confirm that the theory is correct in its identification of two types of vibrational modes for the large-curvature helical limit, and that the succession of these modes is as predicted. No close comparison of measured and predicted frequencies was made, since, as can be seen from the theoretical curves of Figure 11 for α a little greater than 50, these depend quite strongly upon the exact value of α in this range.

7. CONCLUSIONS

Analysis of the equations of free in-plane vibration of a uniformly curved beam with large opening angle has shown that, after the initial rise in non-dimensional eigenvalue and transformation of shape of symmetric modes which occurs at a values of opening angle much less than 2π, a stage of decrease in non-dimensional eigenvalue of all modes follows and continues up to a value of opening angle $\alpha \approx \Lambda_0^{1/4}$, where Λ_0 is non-dimensional eigenvalue of the corresponding mode of a straight beam. These values of opening angle are larger than 2π and at this stage the beam should be considered as a helix. The minimum of non-dimensional

eigenvalue is closely related to the minimum of strain energy, as discussed in sections 3.2 and 5. During the stage of decrease in non-dimensional eigenvalue, the mode shape does not experience significant change.

This stage is followed by a stage of increase in non-dimensional eigenvalues of all modes, which is accompanied by transformation of mode shape. During this stage of transformation, there are two types of vibrational behaviour with quite different mode shapes, in the limit of large opening angle. In the first type, the transverse and tangential displacements are of the same order of magnitude and are highly oscillatory functions, with the number of oscillations proportional to the number of turns in the helix. In the second type, the tangential displacements are of higher orders of magnitude than the transverse ones, and up to the leading order they are slowly varying functions.

Analytic approximations for non-dimensional eigenvalue and mode shape are obtained for both the stage of decrease and the stage of subsequent rise in non-dimensional eigenvalue. A simple rule predicting the type of vibrational behaviour for a particular mode at large values of opening angle has been discussed. Comparison with numerical simulations confirms the validity and satisfactory accuracy of the analytic approximations.

Experiments with curved beams and with helices of small pitch amply confirm the validity of the theoretical predictions, both qualitatively and quantitatively, but this leaves one conundrum to be answered: what is the physical explanation for the two types of behaviour at large opening angles? As noted in Tables 1 and 2, the frequency ordering of mode types at a given curvature is apparently random, though governed by a simple mathematical rule. At the same time it is possible to trace each mode continuously from its initial inextensional small-curvature state out to arbitrarily large curvatures, and it is strange that two neighbouring modes should behave in such different ways. We are unable, at present, to suggest a simple explanation.

Although, in the interests of relative simplicity, this analysis has been confined to the simplest thin-beam approximation and rectangular cross-section, it can be extended by inclusion of shear deformation and rotary inertia effects and to other types of the cross-section. Similar methods of approach can also be used to study the behaviour of beams with non-uniform curvature and cross-section.

ACKNOWLEDGMENT

This work was supported, in part, by a grant from the Australian Research Council.

REFERENCES

1. H. Lamb 1888 *Proceedings of the London Mathematical Society* **19**, 365–376. On the flexure and vibration of a curved bar.

2. J. P. Den Hartog 1928 *Philosophical Magazine* **7**, 400–408. The lowest natural frequency of circular arcs.
3. R. R. Archer 1960 *International Journal of Mechanical Sciences* **1**, 45–56. Small vibrations of thin incomplete circular rings.
4. E. Volterra and J. D. Morell 1960 *ASME Journal of Applied Mechanics* **27**, 744–746. A note on the lowest natural frequency of elastic arcs.
5. E. Volterra and J. D. Morell 1961 *The Journal of the Acoustical Society of America* **33**, 1787–1790. Lowest natural frequencies of elastic hinged arcs.
6. S. Takahashi 1963 *Bulletin of the JSME* **6**, 666–673. Vibration of a circular arc bar in its plane (both ends built-in).
7. M. Petyt and C. C. Fleischer 1971 *Journal of Sound and Vibration*, **18**, 17–30. Free vibration of a curved beam.
8. A. S. Veletos, W. J. Austin, C. A. L. Pereira and S.-J. Wung 1972 *Journal of Engineering Mechanics Division, ASCE* **98**, 311–329. Free in-plane vibration of circular arches.
9. T. Irie, G. Yamada and K. Tanaka 1983 *Journal of Applied Mechanics* **50**, 449–452. Natural frequencies of in-plane vibrations of arcs.
10. P. A. A. Laura and M. J. Maurizi 1987 *The Shock and Vibration Digest* **19**, 6–9. Recent research on vibrations of arch-type structures.
11. P. Chidamparam and A. W. Leissa 1993 *Applied Mechanics Reviews* **46**, 467–483. Vibrations of planar curved beams, rings, and arches.
12. T. Tarnopolskaya, F. de Hoog, N. H. Fletcher and S. Thwaites 1996 *Journal of Sound and Vibration* **196**, 659–680. Asymptotic analysis of the free in-plane vibrations of beams with arbitrarily varying curvature and cross-section.
13. A. Benedetti, L. Deseri and A. Tralli 1996 *Journal of Engineering Mechanics* **122**, 291–299. Simple and effective equilibrium models for vibration analysis of curved rods.
14. T. Tarnopolskaya, F. R. de Hoog and N. H. Fletcher 1999 *Journal of Sound and Vibration* Low-frequency mode transition in the free in-plane vibration of curved beams (in press).
15. S. J. Walsh and R. G. White 1999 *Journal of Sound and Vibration* **221**, 887–902. Mobility of a semi-infinite beam with constant curvature.
16. Y. Kagawa 1968 *Journal of Sound and Vibration* **8**, 1–15. On the dynamical properties of helical springs of finite length with small pitch.
17. A. R. Guido, L. Della Pietra and S. Della Valle 1978 *Meccanica* **13**, 90–108. Transverse vibrations of cylindrical helical springs.
18. L. Della Pietra and S. Della Valle 1982 *Meccanica* **17**, 31–43. On the dynamic behaviour of axially excited helical springs.
19. W. Jiang, W. K. Jones, T. L. Wang and K. H. Wu 1991 *Journal of Applied Mechanics* **58**, 222–228. Free vibrations of helical springs.
20. V. Yildirim 1996 *International Journal for Numerical Methods in Engineering* **39**, 99–114. Investigation of parameters affecting free vibration frequency of helical spring.
21. V. Yildirim and N. Ince, 1997 *Journal of Sound and Vibration* **204**, 311–329. Natural frequencies of helical springs of arbitrary shape.
22. V. Yildirim 1999 *International Journal of Mechanical Sciences* **41**, 919–939. An efficient numerical method for predicting the natural frequencies of cylindrical helical springs.
23. A. E. H. Love 1944 *A Treatise on the Mathematical Theory of Elasticity*. New York: Dover Publications, fourth edition.